Environmental Toxicology and Pharmacology 89 (2022) 103785

Contents lists available at ScienceDirect

Environmental Toxicology and Pharmacology

journal homepage: www.elsevier.com/locate/etap

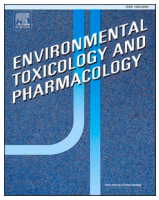

Gestational and lactational xenoestrogen exposure disrupts morphology and inflammatory aspects in mammary gland of gerbil mothers during involution

Thalles Fernando Rocha Ruiz [a,1], Ellen Cristina Rivas Leonel [a,b,1], Simone Jacovaci Colleta [a], Carolina Marques Bedolo [a], Silvana Gisele Pegorin de Campos [a], Sebastião Roberto Taboga [a,*]

[a] Department of Biology, Institute of Biosciences, Humanities and Exact Sciences, São Paulo State University (Unesp), Rua Cristóvão Colombo, 2265, Jardim Nazareth, 15054-000 São José do Rio Preto, São Paulo, Brazil

[b] Department of Histology, Embryology and Cell Biology, Institute of Biological Sciences, Federal University of Goiás (UFG), Avenida Esperança, s/n, Câmpus Samambaia, 74690-900 Goiânia, Goiás, Brazil

ARTICLE INFO

Keywords:
Endocrine disruptor
Bisphenol A
Estradiol
Extracellular matrix
Inflammation

ABSTRACT

In the mammary gland (MG), the developmental window for gestational/lactational differentiation and growth is highly vulnerable to hormonal disruption. Here we describe that the MG involution process in female gerbil mothers is delayed by bisphenol A (BPA) exposure during gestation and lactation. The process is directly influenced by changes in expression of extracellular matrix proteases MMP-2, MMP-9, and FAP, and the incidence of collagen and elastin is reduced after 7 and 14 days of weaning. A pro-inflammatory environment in the late involution process was confirmed by higher expression of TNF-α, COX-2 and phospho-STAT3 n the MG stroma, allied to increases in the incidence of macrophages and mast cells. These aspects impacted the proliferative pattern of epithelial cells, which decreased on the 14th post-weaning day. These data confirm that the milk production window of susceptibility is vulnerable to the impact of BPA, which promotes a suggestive protumoral microenvironment during mammary involution.

1. Introduction

Breast cancer is the most commonly diagnosed type of cancer among women worldwide (Jemal et al., 2011) and its incidence has been related to genetic (Kandel et al., 2021) and epigenetic (Doherty et al., 2010) factors. In addition, environmental compounds have been related to mammary gland neoplastic disturbances; having, for example, a detrimental effect on the expression of hormone receptors in this gland, inducing a mechanism of endocrine disruption (Koual et al., 2020). Disturbances in signaling pathways that impact the epithelium/stroma relation have been widely related to endocrine disruptor exposure, especially in plastic and hormonal responsive glands such as the mammary gland (Wadia et al., 2013). The main concern is triggering of neoplastic development, since this promotes oncogenic transformation in tissues in a short- or long-term manner (Miret et al., 2019).

Exposure to endocrine disruptors that exert estrogenic effects, the xenoestrogens, is ubiquitous. Human biomonitoring guidance values for the chemical bisphenol A (BPA), released by plastics, indicate that 230 μg/L and 135 μg/L of this compound are present in the urine of adults and children, respectively (Ougier et al., 2021). Daily contact with BPA induces toxic impacts, such as metabolic diseases, altered liver function, and estrogen action (vom Saal and Vandenberg, 2021). BPA binds to steroid hormone receptors by an inappropriate transcriptional conformation (Acconcia et al., 2015). As a result, the proliferative mechanisms of estrogen receptors are disturbed, leading to epithelial deregulation and lesions (Durando et al., 2006).

When exposure to endocrine disruptors takes place during the developmental phases of a steroid responsive gland the impacts may be worsened (Colborn et al., 1994). Several research groups have focused on studying the impacts of BPA on mammary gland exposure during windows of susceptibility, such as the perinatal (Altamirano et al., 2017; Gomez et al., 2017; Leonel et al., 2020) and pubertal (Schoeters et al.,

* Correspondence to: São Paulo State University (Unesp), Department of Biology, Institute of Biosciences, Humanities and Exact Sciences, Cristóvão Colombo St., 2265, Postal Code, Jardim Nazareth, 15054–000 São José do Rio Preto, São Paulo, Brazil.
E-mail addresses: thalles.ruiz@unesp.br (T.F.R. Ruiz), ellenleonel@ufg.br (E.C.R. Leonel), Brazil.sebastiao.taboga@unesp.br (S.R. Taboga).
[1] T.F.R. Ruiz and E.C.R. Leonel are joint first authors.

https://doi.org/10.1016/j.etap.2021.103785
Received 15 September 2021; Received in revised form 30 November 2021; Accepted 6 December 2021
Available online 9 December 2021

2008; Wang et al., 2014) developmental phases. This is due to the presence of a dynamic environment in the limits between epithelium and stroma, where a basal membrane rupture is present (Cowin and Wysolmerski, 2010), promoting contact between precursor mammary epithelial cells and BPA in the bloodstream.

Conversely, the impacts of this exposure during adult developmental windows of susceptibility, such as the gestational and lactational proliferative/secreting phases have not been well addressed. This mammary gland stage of development is equally unstable and may provide a hyper exposed environment (Terry et al., 2019). This is because, at this moment, cells are preparing to reorganize and establish a completely developed milk productive gland; consequently, the extracellular matrix undergoes deep changes in its composition and structure (Mori et al., 2013), leaving the cells exposed to serum variations in hormones and disrupting chemicals. The next phase, involution, naturally provides a pro-inflammatory environment that may lead to metastasis and tumor development; thus, previous exposure to disruptors could worsen the risk of developing neoplastic lesions (Faupel-Badger et al., 2012).

It is imperative to understand the impacts on tissue homeostasis during vulnerable initial developmental phases. However, the consequences of this exposure during the mammary gland milk production window of susceptibility have been neglected. Even in rodent models, little is known about what happens to the mothers' mammary gland after exposure to a disrupting environment during the secretory window of susceptibility. Furthermore, impacts may be worsened by mechanisms involved in the gland involution after weaning. Thus, the current work aimed to analyze the morphological features and protein expression in Mongolian gerbil involuting mammary gland from mothers exposed to 17β-estradiol and BPA during the gestational and lactational gland developmental phases.

2. Materials and methods

2.1. Ethics and environment

Female Mongolian gerbils (*Meriones unguiculatus*), a species with a natural tendency to develop mammary neoplasia, were used as an experimental model for endocrine disruption (Ruiz et al., 2021b). Animal experimentation was conducted according to the standards defined by the National Council of Animal Experimentation Control (CONCEA, Brazil, www.mctic.gov.br). The manipulations – gavage, weaning, and euthanasia – were approved by the local Ethics Committee on the Use of Animals (CEUA) (IBILCE/UNESP protocol number 113/2015).

Animals were kept in BPA free isolators (Alesco, Monte Mor, SP, Brazil), organized in racks, with ventilation and a controlled environment: light/dark cycle of 12/12 h, room temperature of 23–26 °C, and 50% relative humidity. Fresh water and a commercial chow (Presence, Paulínia, SP, Brazil) were provided ad libitum during the experiment. Virgin female gerbils were housed with fertile males to mate. Pregnancy was confirmed by the presence of sperm cells in the vaginal smears – pregnancy day 0. The pregnant females were the object of study for this experiment, while the males and the offspring were applied for other experiments.

2.2. Animals and treatments

Pregnant gerbils (N = 34) were divided into four groups and subjected to treatments from the 8th gestational day until the end of lactation (39 days of treatment). The manipulation was always performed during the morning (8–10 a.m.) and was suspended only on the parturition day. All pregnant females were subjected to oral gavage and classified as follows: (Control) daily gavage with vehicle corn oil (Mazola, Mairinque, SP, Brazil); (E2) 35 μg/kg of 17β-estradiol (E8515, Sigma Aldrich, St. Louis, MO, USA), applied as a source of natural occurring estrogen (Kuhl, 2005; Pinkerton et al., 2017; Pinto et al., 2008) diluted in 0.1 ml corn oil 3 times/week; (↓BPA) 50 μg/kg bisphenol A (BPA) (239,658, Sigma Aldrich), safe dose recognized by the European Food Safety Authority, diluted in 0.1 ml corn oil daily (Vandenberg et al. 2012; EFSA, 2015); and (↑BPA) 5000 μg/kg BPA (239,658, Sigma Aldrich) diluted in 0.1 ml corn oil daily, referring to an acute exposure.

After weaning, females from each group were kept with no other treatments and were euthanized on either the 7th or the 14th day post weaning, being sorted into two subgroups (n = 5 animals per subgroup of ↓BPA and ↑BPA; n = 4 animals per subgroup of control; n = 3 animals per subgroup of E2) allowing evaluation of two different periods of mammary gland involution. The euthanasia was performed during the morning and comprised sedation with 3 mg/kg xylazine (Anasedan, Ceva, Paulínia, SP, Brazil) and 10 mg/kg ketamine (Cetamin, Syntec, Barueri, SP, Brazil) followed by decapitation.

2.3. Tissue preparation and morphological analysis

The right abdominal mammary gland was removed and immediately fixed in paraformaldehyde 4% for 24 h at 4 °C. Samples were transferred to ethanol 70% and histologically processed in a semi enclosed system according to standard protocols (TP1020, Leica Biosystems, Buffalo Grove IL, USA). The paraffin blocks obtained were sliced (4 μm thick) and hematoxylin and eosin (HE) staining was conducted. Stained slides were digitally scanned (400 × magnification) using a B× 61VS camera (Olympus Corporation, Tokyo, Japan) coupled to an Olympus VS120 Virtual Microscope Slide Scanning System (VS120–S5) from the same company.

2.4. Tissue general morphology analysis

To evaluate the mammary gland regression process, a first analysis of the gland general morphology was performed. For this, sections from three different depths (40 μm of interval) were evaluated from each animal (OlyVIA 3.2, Olympus). Areas of epithelium, stroma surrounding epithelium (fibroblasts + ECM), and adipose tissue occupation were quantified. A percentage of occupation over the total area of the section was calculated and applied to statistical analysis to infer about the involution process.

2.5. Collagen and elastin fiber quantification

To compare collagen fiber deposition rates in the mammary tissue among groups, picrosirius staining was performed. The slides were stained for 1 h in Sirius Red solution (Direct Red 80 in saturated picric acid solution), washed and counterstained with hematoxylin for 10 min, dehydrated, and mounted. For elastin analysis, the slides were stained using the Weigert's Resorcin-Fuchsin technique, by staining with Resorcin-Fuchsin solution followed by picric acid solution washing. Ten random fields (200x magnification) per animal were evaluated and the area occupied by collagen fibers was quantified automatically by ImageJ software (version 1.52a, Wayne Rasband, NIH, USA).

2.6. Histochemistry and Immunohistochemistry

Sections were dewaxed following standard protocols. Histochemistry was performed for identification of mast cells: sections were stained with 1% toluidine blue (pH 4.0). For immunohistochemistry, antigens were retrieved, endogenous peroxidases were blocked in 5% H_2O_2, and nonspecific proteins were blocked using 5% skimmed milk diluted in TBS. Sections were incubated overnight with the following primary antibodies: α-actin (mouse monoclonal, 1A4, 1:100, sc-32251, Santa Cruz Biotechnology, Dallas, TX, USA), MMP-2 (mouse monoclonal, 8B4, 1:50, sc-13595, Santa Cruz Biotechnology), MMP-9 (mouse monoclonal, 2C3, 1:100, sc-21733, Santa Cruz Biotechnology), FAP (fibroblast activation protein) (mouse monoclonal, F11–24, 1:100, sc-65398, Santa Cruz Biotechnology), Phospho-Stat3 (rabbit monoclonal, 1:100, D3A7,

#9145, Cell Signaling, Danvers, MA, USA), Cox2 (rabbit monoclonal, 1:100, D5H5, #12282, Cell Signaling), F4/80 (rabbit monoclonal, 1:100, D2S9R, #70076, Cell Signaling), TNF-α (rabbit monoclonal, 1:100, D2D4, #11948, Cell Signaling), TGF-β1 (rabbit polyclonal, 3c11, 1:100, sc-146, Santa Cruz Biotechnology), active/cleaved caspase-3 (rabbit polyclonal, 1:100, NB100–56113, Novus Biological, Littleton, CO, USA), and Phospho-Histone H3 (P-H-H3, rabbit polyclonal, H3, 1:75,Ser10, 9701, Cell Signaling). Washes in PBS or TBS were performed between steps. The slides were then incubated with a post-primary antibody and Polymer kit (Novolink ™ polymer detection system 1, Leica Biosystems Newcastle Ltd., Newcastle, United Kingdom) according to the manufacturer's descriptions. Detection of positive staining was performed with 3–30 diaminobenzidine tetrahydrochloride (DAB) (Novolink TM DAB, RE7270-CE, Leica Biosystems, Buffalo Grove, USA) and counterstaining with hematoxylin. Compatibility of the primary antibody in mammary tissue of Mongolian gerbils was confirmed in previous studies (Leonel et al., 2020, 2021; Ruiz et al., 2021a).

2.7. Statistical analysis

Results obtained 7- and 14-days post-weaning were compared in each group by the paired sample T test. The difference between the two correlated samples was evaluated among groups.

To compare the results of each post-weaning period between the groups, the data were checked for normality using the Kolmogorov-Smirnov test. Parametric data (collagen area, PHH3, caspase-3, TGF-β, COX-2, TNF-α, p-STAT3, F4/80, mast cells) were analyzed by one-way ANOVA followed by Tukey's test; non-parametric data (stereological data, elastin area, MMP-2, MMP-9, FAP) were analyzed by the Kruskal-Wallis test followed by Dunn's test. Differences were considered statistically significant when $p < 0.05$. Statistical analyses were performed using GraphPad Prism 5.00 for Windows (GraphPad Software, San Diego, CA, USA, www.graphpad.com).

3. Results

3.1. The morphological features of mammary gland involution were impacted by BPA exposure

The area occupied by epithelial structures in the mammary gland showed a decrease from the 7th to the 14th day in control and E2 groups (Fig. 1a-c). However, mothers treated with BPA presented a lower epithelial occupation area on the 7th day, with no significant reduction from the 7th to 14th day (Fig. 1a).

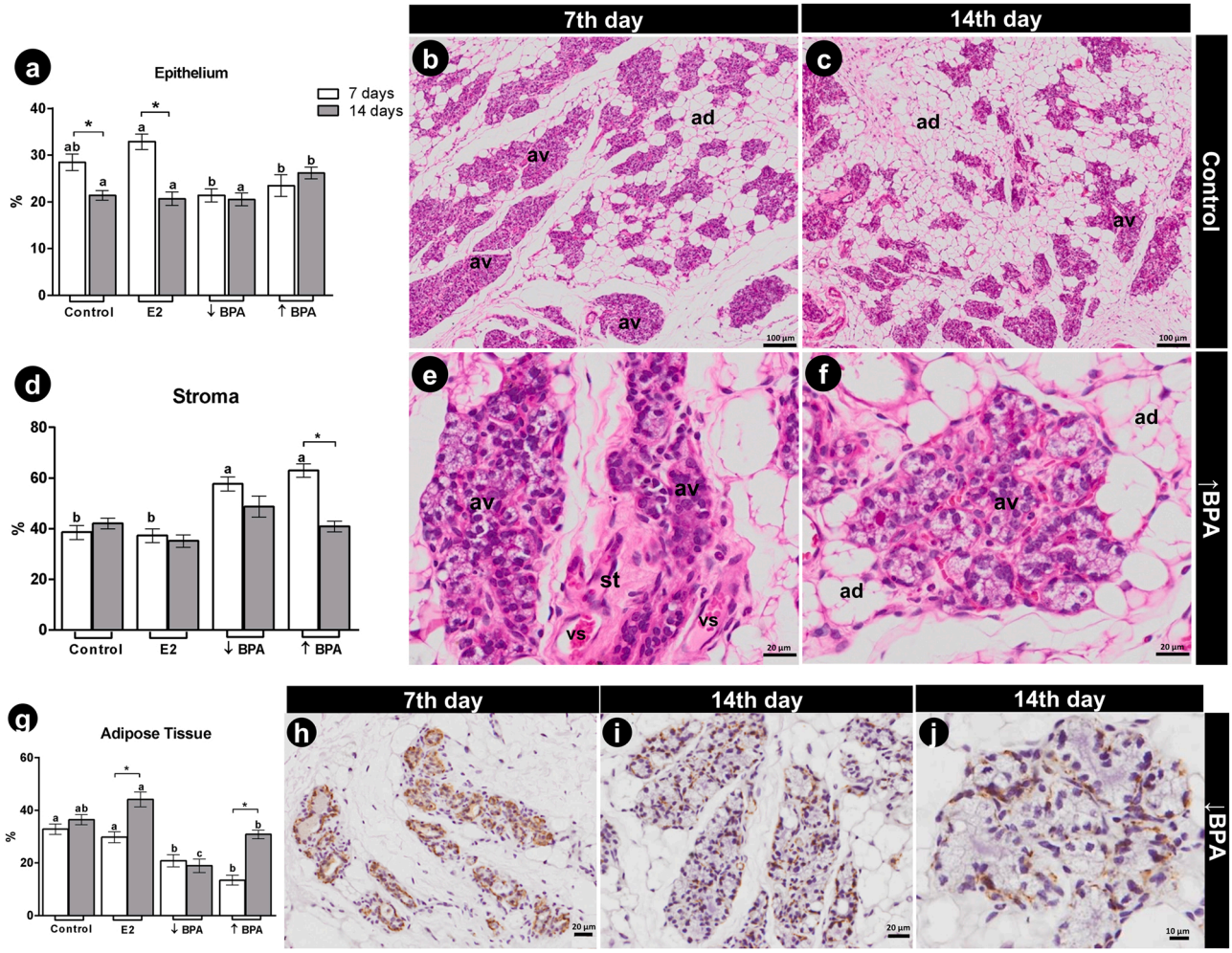

Fig. 1. Morphological features of mammary gland during involution. (a) Percentage of epithelial occupation (mean ± SEM) on 7th and 14th days. Mammary involution from 7th (b) to 14th days (c) in the control group. (d) Stromal area from 7th to14th days of involution. ↑BPA exposure reduced stroma surrounding epithelial structures from 7th (e) to 14th days (f). (g) Adipose tissue area percentage during involution. The appearance of myoepithelial layer thickness, as shown by α-actin staining, changes from the 7th (h) to the 14th (i) post-weaning days, showing a discontinuous pattern on the 14th day (j). Different letters in a, d, and g indicate statistical differences ($p < 0.05$) among groups and * indicate differences between involution periods in the same group (↓BPA and ↑BPA: n = 5 per subgroups; control: n = 4 per subgroups; E2: n = 3 per subgroups). Abbreviations: av: alveoli; ad: adipose tissue; st: stroma; vs: blood vessel. Scale Bars: (b-c) 100 μm; (e-f; h-k) 20 μm; (l) 10 μm.

The non-epithelial compartment was evaluated regarding the occupation rate of adipose tissue and of stroma. Differences in the stromal areas (Fig. 1d) between 7- and 14-days post-lactation were only present in the ↑BPA group (Fig. 1e and f). Both groups treated with BPA showed larger areas of stroma in comparison to all other groups at 7 days post-weaning (Fig. 1 f); no differences between any groups were found for stroma area after 14 days.

The areas of adipose tissue (Fig. 1 g) were larger after 14 days in comparison to 7 days only in the E2 and the ↑BPA treated groups. Both doses of BPA presented a smaller adipose tissue area at 7-days post-weaning in comparison to the control and E2 groups. Control and ↑BPA did not differ statistically at 14 days of involution, whereas ↓BPA was lower in the same period when compared to all groups.

3.2. The thickness and shape of myoepithelial cell layer changed between 7- and 14-days post-weaning

During mammary gland involution, the epithelium acquired a typical morphological aspect that resembles a damaged structure (Fig. 1 h). This is evidenced by α-actin staining for detection of myoepithelial cells. After 14 days, however, alveoli already showed a better-organized structure (Fig. 1i and j). There was a clear reduction in the myoepithelial layer thickness from the 7th to the 14th post-weaning day (Fig. 1 h and j) and the myoepithelial layer showed a discontinuous pattern on the 14th day (Fig. 1j), confirming that at this stage, there was still a clear disruption in the epithelial delimitation that involves the basal layer.

3.3. The incidence of extracellular matrix fibers changed during mammary gland involution

The ECM remodeling was impacted by exposure to BPA and E2. On the 7th day of involution, collagen area percentage (Fig. 2a) was higher in BPA groups compared to control (Fig. 2b and c); at this period, collagen deposition in the E2 group was also higher (Fig. 2d and e) than that of the control. On the 14th day of involution, collagen area in mammary gland exposed to BPA did not differ from the control group (Fig. 2f and g); whereas in the E2 group, it was lower (Fig. 2h and i) compared with all other groups. Elastin area in the ↓BPA group (Fig. 2j) was enhanced in relation to the control group, but there were no differences between ↑BPA and E2 groups and control on the 7th day. On the 14th day of involution, elastin area did not differ among groups. From the 7th to the14th day elastin (Fig. 2k) and collagen presented increased density in the control group, which was not observed in BPA groups. E2 and BPA groups did not present significant differences from 7th to the14th days of involution for elastin fiber area (Fig. 2l-n).

3.4. The expression of MMPs and FAP during mammary gland involution is impacted by BPA exposure

The quantification of ECM remodeling protein expression showed that BPA exposure modulates MMPs and FAP expression in mammary involution. MMP-2 expression (Fig. 3a-d), on the 7th day presented no differences among groups; on the 14th day of involution, MMP-2 expression was slightly increased in the ↑BPA (Fig. 3d) and E2 groups, compared with that in control. On the 7th day MMP-9 expression (Fig. 3e) was low in all treated groups compared to control. Furthermore, the lowest expression of MMP-9 ocurred in ↓BPA and E2 groups on the 7th day. The expression did not change between groups on the 14th day (Fig. 3f and g). From the 7th to 14th days, the MMPs expression decreased only in the control group. while in BPA groups, cells expressing MMPs were spread in stroma surrounding epithelial structures (Fig. 3d and g) and associated to blood vessels.

FAP positive cells (Fig. 3h) were present only in stroma during the involution period. E2 presented drastically increased FAP expression compared to all groups, in both periods of involution (Fig. 3i and j). FAP expression in BPA groups on the 7th and 14th days was lower than E2 but higher than the control group, which presented the lowest rates of FAP expression.

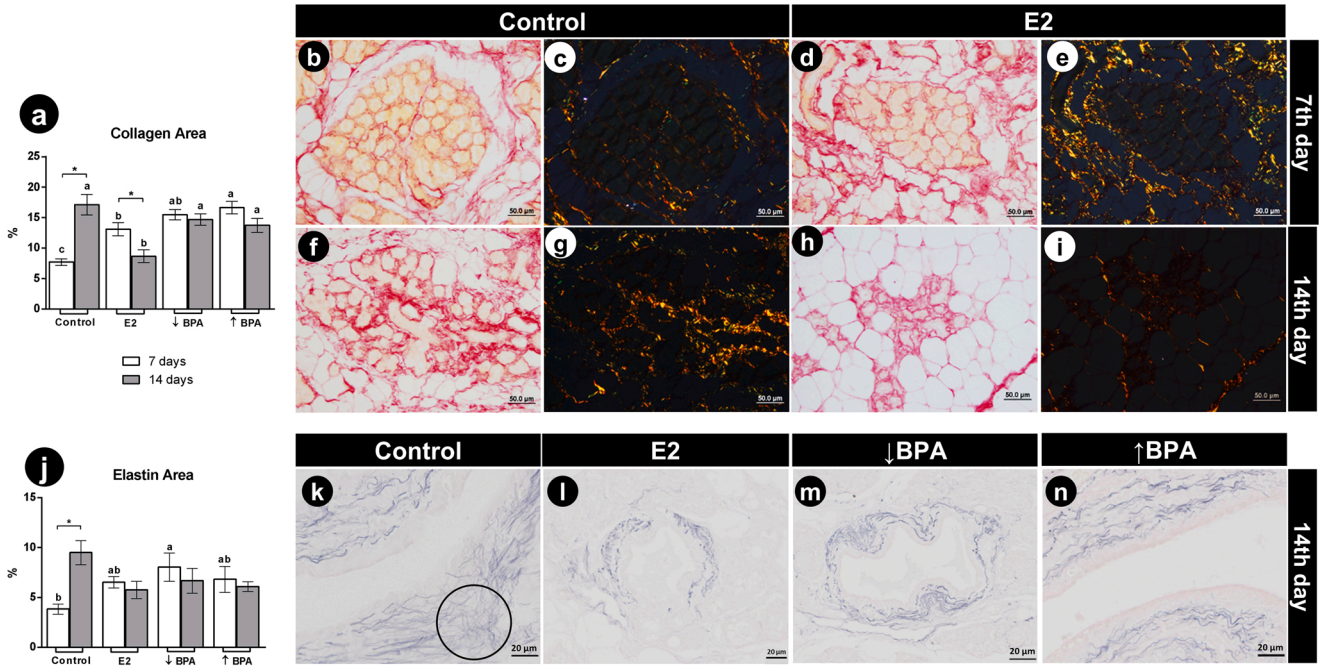

Fig. 2. Extracellular matrix fibers during mammary gland involution. (a) Percentage of collagen area deposition on 7th and 14th days of involution (mean ± SEM). (b-i) Collagen fibers (red). Picrosirius staining demonstrated the collagen deposition at 7 days in control (b, c) and E2 (d, e) groups compared to respective 14 day post-weaning deposition (f, g – control; h, i – E2). (j) Percentage of elastin area on 7th and 14th days of involution (mean ± SEM). (k-n) Resorcin-fucsin staining on 14th day of involution for control (k), E2 (l), ↓BPA (m), and ↑BPA (n) groups. Note the elastin fibers meshwork (circle) in the stroma of the control group (k). Different letters in a and j indicate statistical differences ($p < 0.05$) among groups and * indicate statistical differences between involution periods in the same group (↓BPA and ↑BPA: n = 5 per subgroups; control: n = 4 per subgroups; E2: n = 3 per subgroups). Scale Bars: (b-e; f-i) 50 µm; (k-n) 20 µm.

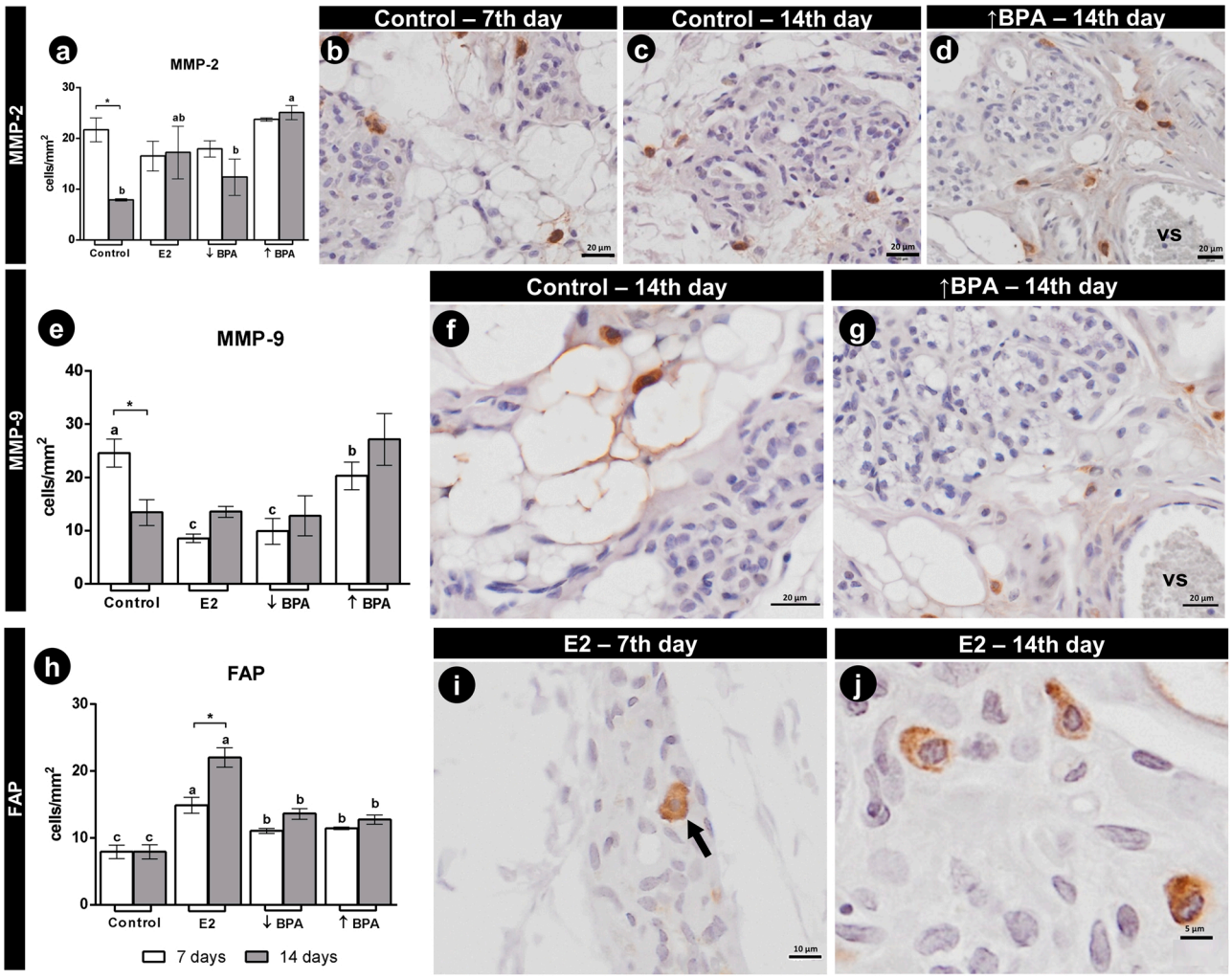

Fig. 3. Extracellular matrix remodeling protein expression during mammary gland involution. MMP-2 (a), MMP-9 (e), and FAP (h) expression (mean of cells/mm2 ± SEM). (b-d) MMP-2 positive cells were found in stoma on 7th (b) and 14th (c) days in control and also in ↑BPA group (d). (f-g) MMP-9 positive cells in adipose tissue in control (f) and perivascular in ↑BPA (g). (i-j) FAP expression: E2 group presented increased expression from 7th (i) to 14th (j) days of involution. Note in (i) the FAP positivity for a mast cell (arrow). Different letters in a, e, and h indicate statistical differences ($p < 0.05$) among groups and * indicate differences between involution periods in the same group (↓BPA and ↑BPA: n = 5 per subgroups; control: n = 4 per subgroups; E2: n = 3 per subgroups). Abbreviation: vs: blood vessel. Scale Bars: (d-i) 20 µm; (j, l) 10 µm; (k) 5 µm.

3.5. The expression of proliferative marker Phospho-Histone H3 was modulated by E2 and BPA exposure

BPA and E2 groups presented high rates of positive cells for PHH3 on the 7th day of involution (Fig. 4a). This scenario changed on the 14th day, when PHH3 expression did not change in the mammary gland of mothers among all groups. Rare PHH3-positive cells were observed in the control group (Fig. 4b). In BPA groups, this proliferative marker was expressed in epithelial (Fig. 4c) and stromal cells (Fig. 4d). The ↓BPA, ↑BPA, and E2 groups showed a decrease in the proliferative activity between the 7th and 14th days of mammary regression, unlike what was observed in the control group, which presented an opposite pattern of PHH3 expression.

3.6. BPA increased TGF-β1 and active Caspase-3 expression in mammary tissue during involution

At 7 days of involution, the number of TGF-β1 positive cells (Fig. 4e) increased in mammary gland of mothers exposed to BPA in comparison to control and E2 groups. Interestingly, this contrast was not maintained on the 14th day of involution, when there were no differences among groups. Only BPA groups and control (Fig. 4f-h) showed differences when comparing 7th to 14th days.

For active caspase-3 (Fig. 4i), BPA groups demonstrated higher rates than control and E2 on the 7th day post-weaning, in which ↑BPA was statistically higher than ↓BPA. Control and E2 groups presented only cytoplasmic staining for caspase-3 (Fig. 4j), whereas BPA groups presented both cytoplasmic and nuclear staining at 7 days (Fig. 4k), and only cytoplasmic staining at 14 days (Fig. 4l). Although a different pattern of intracellular staining was observed, the quantification of positive cells/mm^2 was based on either nuclear or cytoplasmic reaction. From the 7th to the 14th day the number of active caspase-3 positive cells did not change in the control, whereas its expression was reduced in BPA groups and increased in E2 groups.

3.7. BPA and E2 impacted the expression of inflammatory markers during mammary gland involution

Mothers exposed to BPA and E2 presented different expression patterns of inflammatory markers TNFα, COX-2, and p-STAT3. For TNFα (Fig. 5a), control (Fig. 5b) and BPA groups (Fig. 5d) presented lower rates in comparison to the E2 group (Fig. 5c) on the 7th day post-weaning, which showed a high density of positive cells in stroma. This difference was not observed on the 14th day of involution, when none of

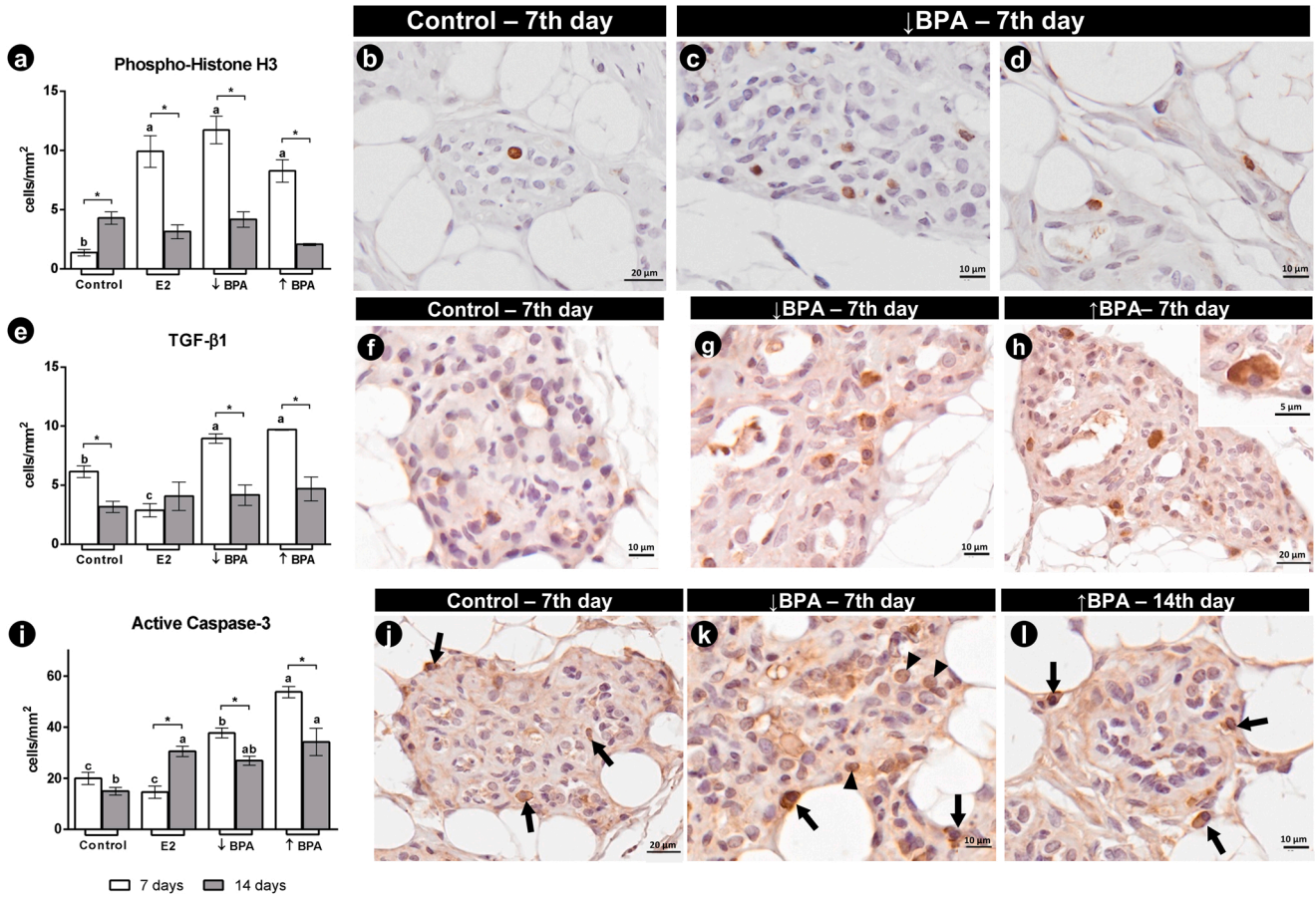

Fig. 4. Proliferative and apoptotic protein expression during mammary gland involution. (a) P-H-H3 positive cells on 7th and 14th days post-weaning (cells/mm2) (mean ± SEM). Control group presented scarce positive cells on 7th day (b); BPA presented epithelial (c) and stromal (d) staining. (e) TGF-β1 positive cells (cells/mm2) (mean ± SEM). Control (f) presented low positivity compared to ↓BPA (g) and ↑BPA (h) on the 7th day. Note that mast cells were stained for TGF-β1 (h-inset). (i) Active caspase-3 positive cells (cells/mm2) (mean ± SEM). At 7-days, the control group presented cytoplasmic staining (arrows) (j), whereas BPA presented cytoplasmic (arrows) and nuclear (arrowheads) staining (k). On the 14th day of involution, only cytoplasmic staining was observed in BPA groups (l). Different letters in a, e, and i indicate statistical differences ($p < 0.05$) among groups and * indicate differences between involution periods in the same group (↓BPA and ↑BPA: n = 5 per subgroups; control: n = 4 per subgroups; E2: n = 3 per subgroups). Scale Bars: (b, h, j) 20 μm; (c, d, f, g, h-inset, k, l) 10 μm.

the groups differed. Furthermore, TNFα positive cells increased in BPA groups from the 7th to 14th days.

COX-2 positive cells (Fig. 5e) presented a higher incidence on the 7th day in the control group (Fig. 5f) which decreased on the 14th day. The expression of COX-2 in mammary gland of mothers exposed to BPA was lower on the 7th day and increased on the 14th day of involution (Fig. 5g-h, respectively). Furthermore, COX-2 did not differ statistically in the E2 group when comparing the 7th and 14th days.

The number of p-STAT3 positive cells (Fig. 5i) remained constant in the control group (Fig. 5j) but was higher on the 7th than 14th day in the E2 group (Fig. 5k). BPA groups showed an increase in the incidence of positive cells between 7 and 14 days of involution (Fig. 5l – ↓BPA; Fig. 5m - ↑BPA). P-STAT3 expression was present as a cytoplasmic and nuclear staining (Fig. 5j-m), which were both considered positive during counts. Lower rates were observed in ↓BPA on the 7th day, when compared to ↑BPA, E2, and control.

3.8. BPA exposure modulated the recruitment of macrophages and mast cells during involution

BPA increased the macrophage population, as shown by F4/80 staining (Fig. 6a), from the 7th to 14th days of involution. Macrophages were scarce in mammary gland tissue on the 7th day in the control (Fig. 6b) and BPA groups and abundant in E2 (Fig. 6c). On the 14th day of involution, ↓BPA presented a high increase in the active macrophage population (Fig. 6d). From the 7th to the 14th days of mammary regression, the macrophage population drastically decreased in E2.

BPA promoted a marked enhancement in mast cell numbers from 7 to 14 days (Fig. 6e). Mast cells in BPA groups were found in epithelial, adipose tissue, and stromal compartments (Fig. 6f, g, and h, respectively). In BPA groups, mast cells were present at intact and degranulated stages. The control group did not present differences between 7 and 14 days. Mast cell recruitment presented opposite modulation in E2 in comparison to BPA, being higher on the 7th than on the 14th day.

4. Discussion

The present experiment revealed that xenoestrogen exposure during the gestational/lactational periods impacts not only neonates', but also the mothers' mammary gland homeostasis in the short-term. Histochemical analysis showed that the normal regression process of the mammary gland is impacted by exposure to BPA and E2, in terms of epithelial and stromal occupation (cells and ECM). Allied to this, the immunohistochemical approach showed that ECM remodeling mechanisms are also impacted by these disruptors in terms of MMPs and FAP expression. Furthermore, indices of cell proliferation and death, as well as inflammatory marker expression, are impacted by this exposure. A schematic representation of the results and discussion is provided in Fig. 7.

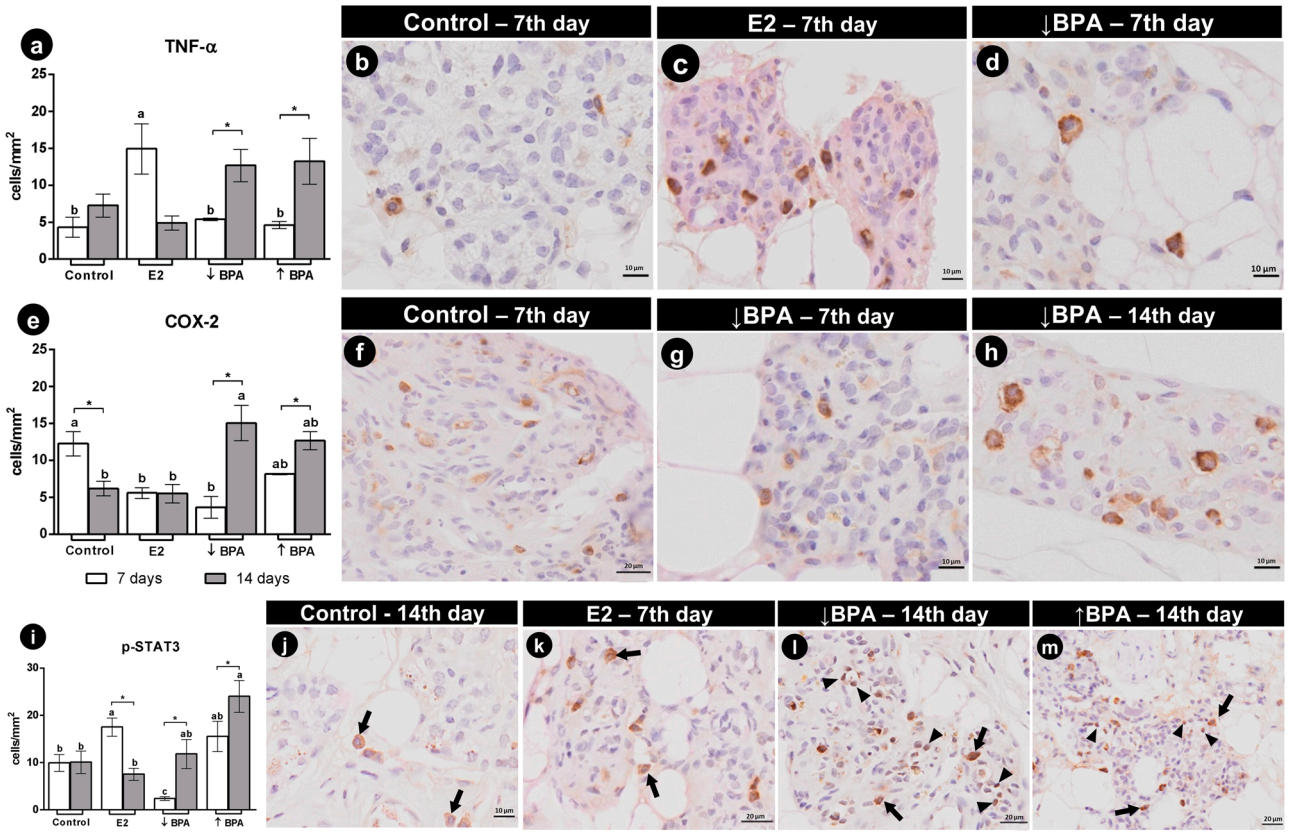

Fig. 5. Inflammatory markers during mammary gland involution. (a) TNFα positive cells (mean ± SEM). On the 7th day, the control group presented low positive cells (b), whereas the E2 group presented high rates of TNFα expression (c). ↓BPA group showed sparse positive cells (d). (e) COX positive cells (mean ± SEM). Control group presented high rates on the 7th day (f). ↓BPA group showed the lowest rates on the 7th day (g), and a drastic increase on the 14th day (h). (i) p-STAT3 expression during involution (mean ± SEM). Arrows indicate stromal cells with cytoplasmic staining in control on the 14th day (j) and E2 on the 7th day (k). Besides stromal cells, ↓BPA (l) and ↑BPA (m) presented epithelial cells with nuclear staining (arrowheads). Different letters in a, e, and i indicate statistical differences ($p < 0.05$) among groups and * indicate differences between involution periods in the same group (↓BPA and ↑BPA: n = 5 per subgroups; control: n = 4 per subgroups; E2: n = 3 per subgroups). Scale Bars: (b, c, g, h, l, m) 10 μm; (d, f, j, k, n, o, p) 20 μm.

4.1. BPA accelerates the mammary gland involution

We have previously described the physiological regression process of Mongolian gerbil mammary gland (Leonel et al., 2017). In that manuscript, the 3rd and 5th post-weaning days were morphologically characterized, and the events of the regression period occurred in a fast manner in comparison to gestational development. One limitation of the present study was that we only analyzed a later period of mammary involution, not describing the possible negative impacts in this first phase (3–5 days post-weaning). These differences could be relevant when associated with exposure to different exogenous estrogenic agents, such as BPA and E2. This relevance is noteworthy in the experimental model applied, which presents neoplasia in hormone-responsive glands and age-related estrogenic sensibilization (Custodio et al., 2008). Based on these results, for better evaluation of the impacts caused by endocrine disruption during gestation and lactation, here we focused on longer involution periods.

The control group showed a reduction in the epithelial compartment between 7 and 14 days, but this was not observed in the BPA groups. This was due to an increase in the apoptotic rate in the epithelial compartment, resulting from high expression of apoptotic proteins such as p-STAT3 and active caspase-3. These proteins are responsible for the initiation of breast involution after milk stasis (Jena et al., 2019), which occurs through the recruitment of phagocytes for tissue remodeling (Hughes et al., 2012) and apoptosis in the epithelial compartment (Chapman et al., 1999; Sargeant et al., 2014).

The second phase of the involution is influenced by the events from the first phase (Hughes and Watson, 2012). At this stage, a physiological ECM remodeling occurs, interfering with the epithelium dynamics and leading to a second apoptotic wave of the compartment (Watson, 2006). E2 exposure led to an epithelial apoptosis delay related to an estrogenic effect (Wärri et al., 2018). However, in the BPA groups, a 2-fold increase was observed in cell death rates in comparison to control. The BPA dose-dependent caspase-3 activity was induced by TGF-β1, which was previously described to establish an apoptotic process (Bailey et al., 2004). This mechanism is often associated with oncogenic activation in tumoral cells (Zhang et al., 2006) supported by an inflammatory microenvironment (Fouad et al., 2014). Our results show that when epithelial cells are subjected to disruption by BPA, they deregulate the cycle by an increase in cell proliferation and in expression of the apoptotic cascade. Thus, it is probable that BPA endocrine deregulation occurs from different cell responses to tissue physiological processes, increasing the sensitivity of mammary gland to hormones and growth factors (Ayyanan et al., 2011; Pupo et al., 2012).

Our results suggest that BPA reprograming of the epithelial cell cycle (Dairkee et al., 2013) extended cell survival time and enhanced lesions, being a hallmark for mammary cancer (Tarullo et al., 2020). In addition, the myoepithelial layer rupture, observed in BPA exposed glands, is an opportunity for invasive ductal carcinoma progression in the mammary gland (Allred et al., 2008). Nevertheless, despite a non-monotonic BPA impact, as previously described (Montévil et al., 2019), p-STAT3 was the main protein that presented different levels of expression in the tissue under low doses of BPA.

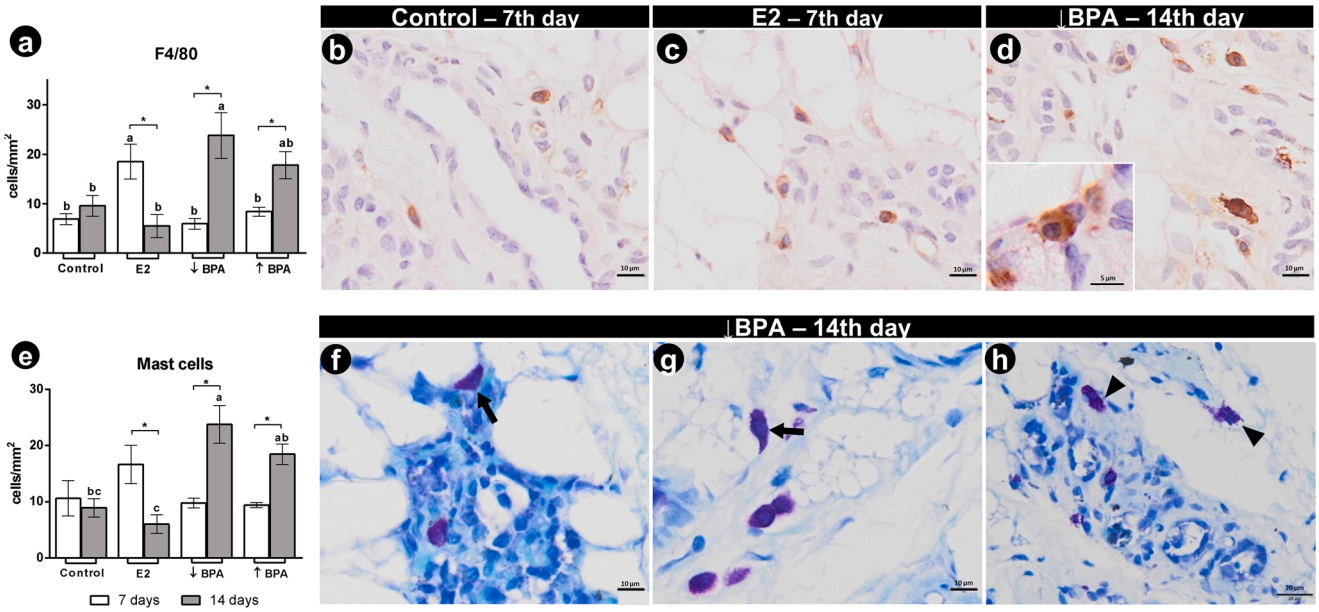

Fig. 6. Macrophage and mast cell incidence during mammary gland involution. (a) Macrophage density (cells/mm2) (mean ± SEM). Macrophages were found in the stromal compartment on the 7th day of involution in control (b) and E2 (c) groups. Macrophage high density was observed in BPA (d) with phagocytic activity in the epithelial compartment (inset). (e) Mast Cell density (cells/mm2) (mean ± SEM). (f-h) Mast cells population: epithelial compartment (f), adipose tissue (g), and in stroma (h). Intact (arrows) and degranulated (arrowheads) mast cells were observed in all compartments. Different letters in a and e indicate statistical differences ($p < 0.05$) among groups and * indicate differences between involution periods in the same group (↓BPA and ↑BPA: n = 5 per subgroups; control: n = 4 per subgroups; E2: n = 3 per subgroups). Scale Bars: (c-g) 10 μm; (h-n) 20 μm.

4.2. BPA alters the stromal compartment and extracellular remodeling proteins in mammary gland during involution

After elimination of epithelial apoptotic cells, stem cells proliferate to reconstruct the epithelium of involuted structures, i.e., terminal-end buds and primary ducts (Maller et al., 2010; Wang et al., 2010). Stroma aids in polarity organization of these cells (Boyd et al., 2007) and is regulated by the estrogenic pathway, which led to a softness condition. Contrarily, findings of BPA groups suggest a stiffness condition. This failure to decrease collagen deposition in mothers treated with BPA may impact the process of breast regression (Simian et al., 2009). Under E2 exposure, ECM softness is promoted by enhanced FAP expression. During involution, fibroblasts and other stromal cells are responsible for the synthesis of proteinases that rearrange the collagen network (Dzięgelewska and Gajewska, 2019). FAP is recognized as a marker for reactive stromal cells (RSC) and carcinoma-associated fibroblasts (CAFs) (Jacob et al., 2012). Despite the absence of differences in the incidence of stroma in the E2 compared to control group, the increase in FAP positive cells may indicate the presence/activation of CAF and RSC, which is favored by the recruitment of macrophages (Tchou et al., 2013). Furthermore, the expression of MMPs in E2 and ↑BPA was supported by higher expression of p-STAT3 (Yuan et al., 2017).

The establishment of a collagen-rich microenvironment in postpartum contribute to pro-tumoral development during breast involution (Provenzano et al., 2006). This invasive condition is promoted by fibrillar collagen, but not by a degraded collagen matrix (Lyons et al., 2011). In the E2 group, however, the presence of FAP determines a degradation activity. The fibrotic phenotype in mammary gland was supported by COX-2 upregulation (Lyons et al., 2011) in BPA groups, mainly on the 14th day of involution.

4.3. BPA aggravates inflammation during mammary gland involution

The expression of inflammatory markers in BPA groups presented an opposite pattern from that observed in control and E2 groups. STAT3 is a first phase marker of mammary gland involution, as previously described (Jena et al., 2019). STAT3 expression is modulated by BPA exposure (Huang et al., 2019) and promotes cell proliferation, typical of breast cancer (Nair et al., 2020). Mammary glands exposed to BPA presented high proliferative activity at 7 days, when p-STAT3 expression was low. However, at 14 days of involution, BPA acts by increasing STAT3 phosphorylation, and hence, decreasing cell proliferation. Of note, BPA exposure can trigger a switch in p-STAT3 and STAT3 expression (Canesi et al., 2005) that could increase the risk of primary breast cancer (Shafei et al., 2018).

E2 is more efficient in binding to estrogen receptors than BPA (Sheehan, 2000). This possibly explains the earlier impacts of E2 exposure (7th day of involution) in the expression of inflammatory markers, being opposite to BPA. The early inflammatory effect promoted by E2 is modulated by TNFα (Xu et al., 2017) and comprises macrophage and mast cell recruitment (Need et al., 2014). However, the significant increase in the incidence of these cells between 7 and 14 days in BPA groups indicates substantial modulation of the inflammatory process (Hennigar et al., 2015), not related to involution. TNFα is a pro-inflammatory cytokine that participates in innate immune response (Perkins, 2007) and is expressed by macrophages when exposed to BPA (Liu et al., 2014).

COX-2 increase in the mammary gland is related to induced-inflammation due to cytokines and hormonal stimuli (Wallace et al., 2019). If its expression is upregulated, it inhibits epithelial cell proliferation and apoptosis (Lu et al., 2005). This inhibition was observed in mammary glands exposed to BPA. In fact, COX-2 is related to chronic inflammation and increases due to high rates of TNFα (Hugo et al., 2015). Post-weaning mammary involution itself is a natural inflammatory microenvironment (Lyons et al., 2011). Thus, enhancement of inflammatory markers represents a risk for post-gestational neoplasia and tumor development (Wallace et al., 2019). Considering this suggestive pro-tumoral microenvironment, BPA modulates the expression and, consequently, the activity of COX-2 in immune-cell recruitment and ECM fibers (Wallace et al., 2019), which may contribute to tumor progression.

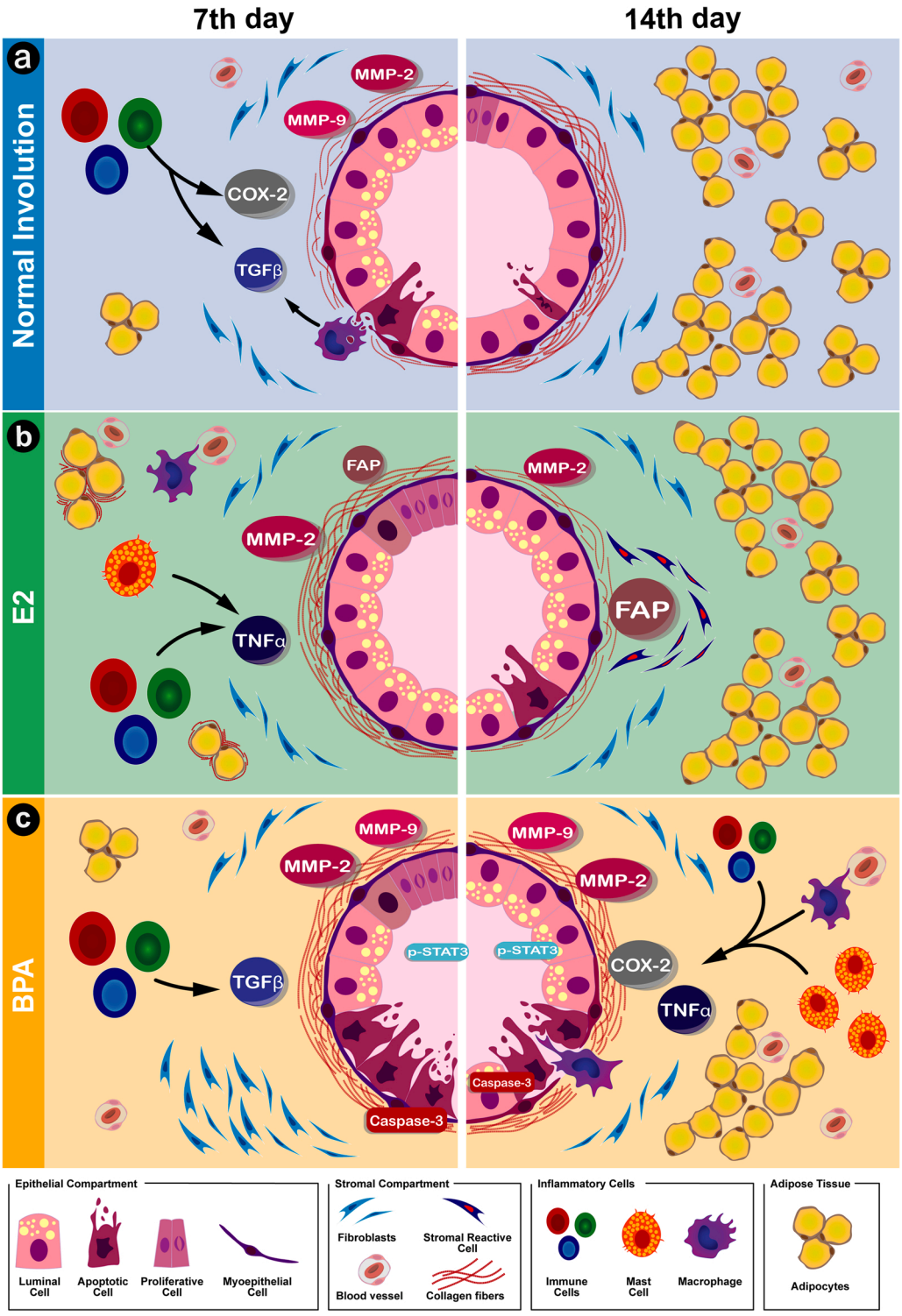

Fig. 7. Morphological features of mammary gland during involution under normal conditions, estradiol, and BPA disruption on 7th and 14th days post-weaning. (a) In a physiological situation, on 7th post-weaning day epithelial cells are apoptotic and stromal cells, such as macrophages and immune cells, express cytokines and COX-2. On the 14th day, the fat pad is reestablished and proliferative activity (PHH3-positive cells) takes place in the epithelial compartment; collagen fibers increase as well. (b) On the 7th day E2 exposure increases proliferation of epithelial cells and the stromal compartment is remodeled by MMP-2, which enhances the expression of TNFα by inflammatory cells, such as mast cells. On the 14th day, E2 induces the presence of apoptotic cells in epithelium and FAP expression in stromal reactive cells. (c) BPA modulates the epithelial compartment through an imbalanced proliferative and apoptotic process on the 7th day, and the stromal compartment is remodeled by MMP-2 and MMP-9. Immune cells express TGFβ in stroma. On the 14th day, TGFβ recruits mast cells, which express COX-2 and TNFα as well as immune cells and macrophages. P-STAT3 is upregulated in both stages in BPA exposed mammary gland.

4.4. BPA recruits mast cells and macrophages during mammary gland involution

Tissue macrophages are recruited in involution to phagocyte the epithelial cells in the apoptotic process, but decrease in number during late involution (Dawson et al., 2020). These cells express MMP-9 (Zollo et al., 2014) in response to the estrogenic pathway, and TNFα, which acts as a signal for new recruitment and activation of pro-inflammatory cells (Fleming et al., 2012). E2 stimulated the recruitment of macrophages on the 7th day. Contrarily, BPA showed a late effect, related to the increase in TNFα from 7th to the 14th day. Another factor that could contribute to macrophage infiltration in BPA groups is the high expression of p-STAT3 (Stein et al., 2003). STAT3 expression changed in ↓BPA and ↑BPA groups from the 7th to 14th day and could stimulate this infiltration by the cited pathway. These inflammatory features and expression of MMPs contribute to create and amplify a suggestive tumorigenic microenvironment by enhancing the macrophage population in BPA groups (Fleming et al., 2012; Xu, 2017).

TGF-β1 is a chemotactic protein for monocytes (Zollo et al., 2014) and mast cells (Ramírez-Valadez et al., 2017). The increased expression

in BPA groups on the 7th day of mammary gland involution was followed by a drastic enhancement in these cell numbers on the 14th day. Elgert and colleagues (1998) associated the loss of antitumoral macrophage activity with TGF-β1 enhancement in tissue, similarly to the mammary gland microenvironment described here on the 7th day in BPA groups. These macrophages could contribute to cancer progression and are found early in breast tumors (Dawson et al., 2020). Tumor-associated macrophages (TAMs) are a myeloid cell type recruited by the tumor site to produce an inflammatory microenvironment for cancer progression and metastasis (Mao et al., 2018; Wani et al., 2014). In the present study, BPA groups showed a correlation of chemoattractant protein TGF-β1 on the 7th day, which allowed the infiltration of TAMs. p-STAT3 in turn supported their recruitment and activation (Clarkson et al., 2006), as observed by the enhancement in COX-2 expression (Gan et al., 2016).

Mast cells trigger the interaction between epithelium and stromal compartments (Durando et al., 2006) and stimulate proliferation in ductal epithelium and the development of carcinoma in situ. Both events were observed in BPA groups during involution (7th to 14th day). As discussed above, the proliferative-apoptotic balance of involution is impaired by BPA exposure and has been deployed in a suggestive preneoplastic and inflammatory microenvironment. Furthermore, the increase in TNFα expression in the E2 group explains the reduction in mast cell numbers, since this is a cytokine that regulates the local degranulation of mast cells in involution (Ramirez et al., 2012).

Exposure to E2 induces a pro-invasive microenvironment, while BPA promotes a fibrotic and inflammatory phenotype. Even though BPA and E2 act in similar pathways, our study showed that inflammatory responses – i.e., recruitment of mast cells and macrophages, proliferation/apoptosis – were opposite between 7 and 14 days of involution. Thus, compared to E2, BPA acts in several other pathways to alter the normal and synthetic-sensitized tissue. This evidence brings to light a perspective for future analysis: estrogenic receptor expression could unveil much of what is still to be clarified, since their affinity varies according to the estrogenic compound. Exposure during the pregnancy and lactation windows of susceptibility induce a progression of features related to the increase in breast cancer incidence (Shafei et al., 2018). BPA exposure contributes to different types of breast cancer (Engin and Engin, 2021) and neoplasia (Sprague et al., 2013) development. The exposure period of the present study should be taken into consideration as a trigger point of pro-tumoral establishment.

5. Conclusion

Gestational and lactational exposure to BPA appears to be crucial for progression of a suggestive pro-tumoral feature and microenvironment of mammary gland, which potentially aggravate the risks of cancer development. The epithelium and stroma of mammary gland during regression (Fig. 7a) negatively respond to E2 (Fig. 7b) and BPA (Fig. 7c) exposure. This pro-tumoral microenvironment is depicted by variations in cell death and proliferation indices and in expression of inflammatory markers, which promote a favorable cancer microenvironment.

Compliance and Ethical Standard

Ethical approval

Experiments adhered to guidelines established by the National Council of Animal Experiment Control (CONCEA, Brazil, www.mctic.gov.br) and were approved by the committee for animal care of the Ethics Committee on the Use of Animals (CEUA) (IBILCE/UNESP protocol number 113/2015).

Funding Sources

This work was supported by the Fundaç ão de Amparo à Pesquisa do Estado de São Paulo – FAPESP (Master fellowship to T.F.R. Ruiz, 2020/01240–9; and research financing, 2018/23383–6); Coordenaç ão de Aperfeiçoamento de Pessoal de N í vel Superior – CAPES (finance code 001); and the National Council for Scientific and Technological Development (CNPq) (Grant Number: 302938/2020/6).

CRediT authorship contribution statement

T.F.R. Ruiz and E.C.R. Leonel contributed equally to this manuscript in the following actions: study conceptualization and methodology, formal analysis, investigation, resources, data curation and writing of both, original draft, and review/editing. S.V. Colleta: investigation, resources, data curation. C.M. Bedolo: formal analysis, investigation, resources, data curation. S.G.P. Campos: writing - original draft, data curation and investigation. S.R. Taboga: conceptualization and methodology, writing - original draft, supervision, project administration and funding acquisition.

Declaration of Competing Interest

The authors declare the following financial interests/personal relationships which may be considered as potential competing interests: Leonel E.C.R reports financial support was provided by Coordination of Higher Education Personnel Improvement. Ruiz T.F.R. reports financial support was provided by State of Sao Paulo Research Foundation. Taboga S.R. reports financial support was provided by State of Sao Paulo Research Foundation. Taboga S.R. reports financial support was provided by National Council for Scientific and Technological Development.

Acknowledgements

The authors would like to thank MSc. Luiz Roberto Falleiros for technical assistance during the development of the experiments.

Funding Information

Fundaç ão de Amparo à Pesquisa do Estado de São Paulo – FAPESP (Master fellowship to T.F.R. Ruiz, 2020/01240–9; and research financing, 2018/23383–6) and Coordenaç ão de Aperfeiçoamento de Pessoal de N í vel Superior – CAPES (finance code 001).

Conflict of Interest

The authors declare that there is no conflict of interest.

References

Acconcia, F., Pallottini, V., Marino, M., 2015. Molecular mechanisms of action of BPA. Dose-Response 13, 1–9. https://doi.org/10.1177/1559325815610582.

Allred, D.C., Wu, Y., Mao, S., Nagtegaal, I.D., Lee, S., Perou, C.M., Mohsin, S.K., O'Connell, P., Tsimelzon, A., Medina, D., 2008. Ductal carcinoma in situ and the emergence of diversity during breast cancer evolution. Clin. Cancer Res. 14, 370–378. https://doi.org/10.1158/1078-0432.CCR-07-1127.

Altamirano, G.A., Ramos, J.G., Gomez, A.L., Luque, E.H., Muñoz-de-Toro, M., Kass, L., 2017. Perinatal exposure to bisphenol A modifies the transcriptional regulation of the β-casein gene during secretory activation of the rat mammary gland. Mol. Cell. Endocrinol. 439, 407–418. https://doi.org/10.1016/j.mce.2016.09.032.

Ayyanan, A., Laribi, O., Schuepbach-Mallepell, S., Schrick, C., Gutierrez, M., Tanos, T., Lefebvre, G., Rougemont, J., Yalcin-Ozuysal, Ö., Brisken, C., 2011. Perinatal exposure to bisphenol A increases adult mammary gland progesterone response and cell number. Mol. Endocrinol 25, 1915–1923. https://doi.org/10.1210/me.2011-1129.

Bailey, J.P., Nieport, K.M., Herbst, M.P., Srivastava, S., Serra, R.A., Horseman, N.D., 2004. Prolactin and transforming growth factor-β signaling exert opposing effects on mammary gland morphogenesis, involution, and the Akt-forkhead pathway. Mol. Endocrinol. 18, 1171–1184. https://doi.org/10.1210/me.2003-0345.

Boyd, N.F., Guo, H., Martin, L.J., Sun, L., Stone, J., Fishell, E., Jong, R.A., Hislop, G., Chiarelli, A., Minkin, S., Yaffe, M.J., 2007. Mammographic density and the risk and detection of breast cancer. N. Engl. J. Med. 356, 227–236. https://doi.org/10.1056/NEJMoa062790.

Canesi, L., Betti, M., Lorusso, L.C., Ciacci, C., Gallo, G., 2005. “In vivo” effects of bisphenol A in Mytilus hemocytes: Modulation of kinase-mediated signalling pathways. Aquat. Toxicol. 71, 73–84. https://doi.org/10.1016/j.aquatox.2004.10.011.

Chapman, R.S., Lourenco, P.C., Tonner, E., Flint, D.J., Selbert, S., Takeda, K., Akira, S., Clarke, A.R., Watson, C.J., 1999. Suppression of epithelial apoptosis and delayed mammary gland involution in mice with a conditional knockout of Stat3. Genes Dev. 13, 2604–2616. https://doi.org/10.1101/gad.13.19.2604.

Clarkson, R.W.E., Boland, M.P., Kritikou, E.A., Lee, J.M., Freeman, T.C., Tiffen, P.G., Watson, C.J., 2006. The genes induced by signal transducer and activators of transcription (STAT)3 and STAT5 in mammary epithelial cells define the roles of these STATs in mammary development. Mol. Endocrinol. 20, 675–685. https://doi.org/10.1210/me.2005-0392.

Colborn, T., vom Saal, F.S., Soto, A.M., 1994. Developmental effects of endocrine-disrupting chemicals in wildlife and humans. Environ. Impact Assess. Rev. 14, 469–489. https://doi.org/10.1016/0195-9255(94)90014-0.

Cowin, P., Wysolmerski, J., 2010. Molecular mechanisms guiding embryonic mammary gland development. Cold Spring Harb. Perspect. Biol. 2 https://doi.org/10.1101/cshperspect.a003251.

Custodio, A.M.G., Santos, F.C.A., Campos, S.G.P., Vilamaior, P.S.L., Góes, R.M., Taboga, S.R., 2008. Aging effects on the mongolian gerbil female prostate (Skene’s paraurethral glands): Structural, ultrastructural, quantitative, and hormonal evaluations. Anat. Rec. 291, 463–474. https://doi.org/10.1002/ar.20637.

Dairkee, S.H., Luciani-Torres, M.G., Moore, D.H., Goodson, W.H., 2013. Bisphenol-A-induced inactivation of the p53 axis underlying deregulation of proliferation kinetics, and cell death in non-malignant human breast epithelial cells. Carcinogenesis 34, 703–712. https://doi.org/10.1093/carcin/bgs379.

Dawson, C.A., Pal, B., Vaillant, F., Gandolfo, L.C., Liu, Z., Bleriot, C., Ginhoux, F., Smyth, G.K., Lindeman, G.J., Mueller, S.N., Rios, A.C., Visvader, J.E., 2020. Tissue-resident ductal macrophages survey the mammary epithelium and facilitate tissue remodelling. Nat. Cell Biol. 22, 546–558. https://doi.org/10.1038/s41556-020-0505-0.

Doherty, L.F., Bromer, J.G., Zhou, Y., Aldad, T.S., Taylor, H.S., 2010. In utero exposure to diethylstilbestrol (DES) or bisphenol-A (BPA) increases EZH2 expression in the mammary gland: An epigenetic mechanism linking endocrine disruptors to breast cancer. Horm. Cancer 1, 146–155. https://doi.org/10.1007/s12672-010-0015-9.

Durando, M., Kass, L., Piva, J., Sonnenschein, C., Soto, A.M., Luque, E.H., Muñoz-De-Toro, M., 2006. Prenatal bisphenol a exposure induces preneoplastic lesions in the mammary gland in wistar rats. Environ. Health Perspect. 115, 80–86. https://doi.org/10.1289/ehp.9282.

Dzięgelewska, Ż., Gajewska, M., 2019. Stromal-epithelial interactions during mammary gland development. Stromal Cells - Struct. Funct. Ther. Implic. https://doi.org/10.5772/intechopen.80405.

EFSA, 2015. Scientific Opinion on the risks to public health related to the presence of bisphenol A (BPA) in foodstuffs. EFSA J. 13 https://doi.org/10.2903/j.efsa.2015.3978.

Elgert, K.D., Alleva, D.G., Mullins, D.W., 1998. Tumor-induced immune dysfunction: The macrophage connection. J. Leukoc. Biol. 64, 275–290. https://doi.org/10.1002/jlb.64.3.275.

Engin, A.B., Engin, A., 2021. The effect of environmental bisphenol A exposure on breast cancer associated with obesity. Environ. Toxicol. Pharmacol. 81, 103544 https://doi.org/10.1016/j.etap.2020.103544.

Faupel-Badger, J.M., Arcaro, K.F., Balkam, J.J., Eliassen, A.H., Hassiotou, F., Lebrilla, C. B., Michels, K.B., Palmer, J.R., Schedin, P., Stuebe, A.M., Watson, C.J., Sherman, M. E., 2012. Postpartum remodeling, lactation, and breast cancer risk: summary of a national cancer institute–Sponsored Workshop. JNCI J. Natl. Cancer Inst. 105, 166–174. https://doi.org/10.1093/jnci/djs505.

Fleming, J.M., Miller, T.C., Kidacki, M., Ginsburg, E., Stuelten, C.H., Stewart, D.A., Troester, M.A., Vonderhaar, B.K., 2012. Paracrine interactions between primary human macrophages and human fibroblasts enhance murine mammary gland humanization in vivo. Breast Cancer Res. 14, 1–18. https://doi.org/10.1186/bcr3215.

Fouad, T.M., Kogawa, T., Reuben, J.M., Ueno, N.T., 2014. The role of inflammation in inflammatory breast cancer. Int. J. Radiat. Biol. 53–73. https://doi.org/10.1007/978-3-0348-0837-8_3.

Gan, L., Qiu, Z., Huang, J., Li, Y., Huang, H., Xiang, T., Wan, J., Hui, T., Lin, Y., Li, H., Ren, G., 2016. Cyclooxygenase-2 in tumor-associated macrophages promotes metastatic potential of breast cancer cells through akt pathway. Int. J. Biol. Sci. 12, 1533–1543. https://doi.org/10.7150/ijbs.15943.

Gomez, A.L., Delconte, M.B., Altamirano, G.A., Vigezzi, L., Bosquiazzo, V.L., Barbisan, L. F., Ramos, J.G., Luque, E.H., Muñoz-de-Toro, M., Kass, L., 2017. Perinatal exposure to bisphenol a or diethylstilbestrol increases the susceptibility to develop mammary gland lesions after estrogen replacement therapy in middle-aged rats. Horm. Cancer 8, 78–89. https://doi.org/10.1007/s12672-016-0282-1.

Hennigar, S.R., Velasquez, V., Kelleher, S.L., 2015. Obesity-induced inflammation is associated with alterations in subcellular zinc pools and premature mammary gland involution in lactating mice. J. Nutr. 145, 1999–2005. https://doi.org/10.3945/jn.115.214122.

Huang, F.M., Chang, Y.C., Lee, S.S., Yang, M.L., Kuan, Y.H., 2019. Expression of pro-inflammatory cytokines and mediators induced by Bisphenol A via ERK-NFκB and JAK1/2-STAT3 pathways in macrophages. Environ. Toxicol. 34, 486–494. https://doi.org/10.1002/tox.22702.

Hughes, K., Watson, C.J., 2012. The role of Stat3 in mammary gland involution: cell death regulator and modulator of inflammation. Horm. Mol. Biol. Clin. Investig. 10, 211–215. https://doi.org/10.1515/hmbci-2012-0008.

Hughes, K., Wickenden, J.A., Allen, J.E., Watson, C.J., 2012. Conditional deletion of Stat3 in mammary epithelium impairs the acute phase response and modulates immune cell numbers during post-lactational regression. J. Pathol. 227, 106–117. https://doi.org/10.1002/path.3961.

Hugo, H.J., Saunders, C., Ramsay, R.G., Thompson, E.W., 2015. New insights on COX-2 in chronic inflammation driving breast cancer growth and metastasis. J. Mammary Gland Biol. Neoplasia 20, 109–119. https://doi.org/10.1007/s10911-015-9333-4.

Jacob, M., Chang, L., Pure, E., 2012. Fibroblast activation protein in remodeling tissues. Curr. Mol. Med. 12, 1220–1243. https://doi.org/10.2174/156652412803833607.

Jemal, A., Bray, F., Center, M.M., Ferlay, J., Ward, E., Forman, D., 2011. Global cancer statistics. CA. Cancer J. Clin. 61, 69–90. https://doi.org/10.3322/caac.20107.

Jena, M.K., Jaswal, S., Kumar, S., Mohanty, A.K., 2019. Molecular mechanism of mammary gland involution: An update. Dev. Biol. 445, 145–155. https://doi.org/10.1016/j.ydbio.2018.11.002.

Kandel, A., Dhillon, S.K., Prabaharan, C.B., Fatnin Binti Hisham, S., Rajamanickam, K., Napper, S., Chidambaram, S.B., Essa, M.M., Yang, J., Sakharkar, M.K., 2021. Identifying kinase targets of PPARγ in human breast cancer. J. Drug Target. 1–18. https://doi.org/10.1080/1061186X.2021.1877719.

Koual, M., Tomkiewicz, C., Cano-Sancho, G., Antignac, J.P., Bats, A.S., Coumoul, X., 2020. Environmental chemicals, breast cancer progression and drug resistance. Environ. Heal. A Glob. Access Sci. Source 19, 1–25. https://doi.org/10.1186/s12940-020-00670-2.

Kuhl, H., 2005. Pharmacology of estrogens and progestogens: influence of different routes of administration. Climacteric 8, 3–63. https://doi.org/10.1080/13697130500148875.

Leonel, E.C.R., Campos, S.G.P., Bedolo, C.M.B., Guerra, L.H.A., Vilamaior, P.S.L., Calmon, M.F., Rahal, P., Amorim, C.A., Taboga, S.R., 2020. Perinatal exposure to bisphenol A impacts in the mammary gland morphology of adult Mongolian gerbils. Exp. Mol. Pathol. 113, 104374 https://doi.org/10.1016/j.yexmp.2020.104374.

Leonel, E.C.R., Ruiz, T.F.R., Bedolo, C.M., Campos, S.G.P., Taboga, S.R., 2021. Inflammatory repercussions in female steroid responsive glands after perinatal exposure to bisphenol A and 17–β estradiol. Cell Biol. Int. https://doi.org/10.1002/cbin.11665.

Leonel, E.C.R.R., Falleiros, L.R., Campos, S.G.P.P., Taboga, S.R., 2017. Histological and immunohistochemical characterization of the Mongolian gerbil’s mammary gland during gestation, lactation and involution. Acta Histochem. 119, 273–283. https://doi.org/10.1016/j.acthis.2017.02.003.

Liu, Y., Mei, C., Liu, H., Wang, H., Zeng, G., Lin, J., Xu, M., 2014. Modulation of cytokine expression in human macrophages by endocrine-disrupting chemical Bisphenol-A. Biochem. Biophys. Res. Commun. 451, 592–598. https://doi.org/10.1016/j.bbrc.2014.08.031.

Lu, S., Yu, G., Zhu, Y., Archer, M.C., 2005. Cyclooxygenase-2 overexpression in MCF-10F human breast epithelial cells inhibits proliferation, apoptosis and differentiation, and causes partial transformation. Int. J. Cancer 116, 847–852. https://doi.org/10.1002/ijc.21142.

Lyons, T.R., O’Brien, J., Borges, V.F., Conklin, M.W., Keely, P.J., Eliceiri, K.W., Marusyk, A., Tan, A.C., Schedin, P., 2011. Postpartum mammary gland involution drives progression of ductal carcinoma in situ through collagen and COX-2. Nat. Med. 17, 1109–1116. https://doi.org/10.1038/nm.2416.

Maller, O., Martinson, H., Schedin, P., 2010. Extracellular matrix composition reveals complex and dynamic stromal-epithelial interactions in the mammary gland. J. Mammary Gland Biol. Neoplasia 15, 301–318. https://doi.org/10.1007/s10911-010-9189-6.

Mao, S.P.H., Park, M., Cabrera, R.M., Christin, J.R., Karagiannis, G.S., Oktay, M.H., Zaiss, D.M.W., Abrams, S.I., Guo, W., Condeelis, J.S., Kenny, P.A., Segall, J.E., 2018. Loss of amphiregulin reduces myoepithelial cell coverage of mammary ducts and alters breast tumor growth. Breast Cancer Res. 20, 1–14. https://doi.org/10.1186/s13058-018-1057-0.

Miret, N.V., Pontillo, C.A., Zárate, L.V., Kleiman de Pisarev, D., Cocca, C., Randi, A.S., 2019. Impact of endocrine disruptor hexachlorobenzene on the mammary gland and breast cancer: The story thus far. Environ. Res. 173, 330–341. https://doi.org/10.1016/j.envres.2019.03.054.

Montévil, M., Acevedo, N., Schaeberle, C.M., Bharadwaj, M., Fenton, S.E., Soto, A.M., 2019. A combined morphometric and statistical approach to assess non-monotonicity in the developing mammary gland of rats in the CLARITY-BPA study. bioRxiv 2012, 1–21. https://doi.org/10.1101/783019.

Mori, H., Lo, A.T., Inman, J.L., Alcaraz, J., Ghajar, C.M., Mott, J.D., Nelson, C.M., Chen, C.S., Zhang, H., Bascom, J.L., Seiki, M., Bissell, M.J., 2013. Transmembrane/cytoplasmic, rather than catalytic, domains of Mmp14 signal to MAPK activation and mammary branching morphogenesis via binding to integrin β1. Development 140, 343–352. https://doi.org/10.1242/dev.084236.

Nair, V.A., Valo, S., Peltomäki, P., Bajbouj, K., Abdel-Rahman, W.M., 2020. Oncogenic potential of bisphenol a and common environmental contaminants in human mammary epithelial cells. Int. J. Mol. Sci. 21 https://doi.org/10.3390/ijms21103735.

Need, E.F., Atashgaran, V., Ingman, W.V., Dasari, P., 2014. Hormonal regulation of the immune microenvironment in the mammary gland. J. Mammary Gland Biol. Neoplasia 19, 229–239. https://doi.org/10.1007/s10911-014-9324-x.

Ougier, E., Zeman, F., Antignac, J.P., Rousselle, C., Lange, R., Kolossa-Gehring, M., Apel, P., 2021. Human biomonitoring initiative (HBM4EU): Human biomonitoring guidance values (HBM-GVs) derived for bisphenol A. Environ. Int. 154, 106563 https://doi.org/10.1016/j.envint.2021.106563.

Perkins, N.D., 2007. Integrating cell-signalling pathways with NF-κB and IKK function. Nat. Rev. Mol. Cell Biol. 8, 49–62. https://doi.org/10.1038/nrm2083.

Pinkerton, J.A.V., Aguirre, F.S., Blake, J., Cosman, F., Hodis, H., Hoffstetter, S., Kaunitz, A.M., Kingsberg, S.A., Maki, P.M., Manson, J.A.E., Marchbanks, P.,

McClung, M.R., Nachtigall, L.E., Nelson, L.M., Pace, D.T., Reid, R.L., Sarrel, P.M., Shifren, J.L., Stuenkel, C.A., Utian, W.H., 2017. The 2017 hormone therapy position statement of the North American Menopause Society. Menopause 24, 728–753. https://doi.org/10.1097/GME.0000000000000921.

Pinto, M.E., Vilamaior, P.S.L., Taboga, S.R., Góes, R.M., 2008. Exposure of young rats to high estrogen doses leads to degeneration of elongated spermatids. Tissue Cell 40, 31–42. https://doi.org/10.1016/j.tice.2007.09.002.

Provenzano, P.P., Eliceiri, K.W., Campbell, J.M., Inman, D.R., White, J.G., Keely, P.J., 2006. Collagen reorganization at the tumor-stromal interface facilitates local invasion. BMC Med 4, 1–15. https://doi.org/10.1186/1741-7015-4-38.

Pupo, M., Pisano, A., Lappano, R., Santolla, M.F., de Francesco, E.M., Abonante, S., Rosano, C., Maggiolini, M., 2012. Bisphenol A induces gene expression changes and proliferative effects through GPER in breast cancer cells and cancer-associated fibroblasts. Environ. Health Perspect. 120, 1177–1182. https://doi.org/10.1289/ehp.1104526.

Ramírez-Valadez, K.A., Vázquez-Victorio, G., Macías-Silva, M., González-Espinosa, C., 2017. Fyn kinase mediates cortical actin ring depolymerization required for mast cell migration in response to TGF-β in mice. Eur. J. Immunol. 47, 1305–1316. https://doi.org/10.1002/eji.201646876.

Ramirez, R.A., Lee, A., Schedin, P., Russell, J.S., Masso-Welch, P.A., 2012. Alterations in mast cell frequency and relationship to angiogenesis in the rat mammary gland during windows of physiologic tissue remodeling. Dev. Dyn. 241, 890–900. https://doi.org/10.1002/dvdy.23778.

Ruiz, T.F.R., Colleta, S.J., Leonel, E.C.R., Taboga, S.R., 2021a. Mammary carcinoma in aged gerbil mothers after endocrine disruption in pregnancy and lactation. Endocr. Relat. Cancer. https://doi.org/10.1530/ERC-21-0198.

Ruiz, T.F.R., Colleta, S.J., Zuccari, D.A.P., de, C., Vilamaior, P.S.L., Leonel, E.C.R., Taboga, S.R., 2021b. Hormone receptor expression in aging mammary tissue and carcinoma from a rodent model after xenoestrogen disruption. Life Sci 285, 120010. https://doi.org/10.1016/j.lfs.2021.120010.

Sargeant, T.J., Lloyd-Lewis, B., Resemann, H.K., Ramos-Montoya, A., Skepper, J., Watson, C.J., 2014. Stat3 controls cell death during mammary gland involution by regulating uptake of milk fat globules and lysosomal membrane permeabilization. Nat. Cell Biol. 16, 1057–1068. https://doi.org/10.1038/ncb3043.

Schoeters, G., Den Hond, E., Dhooge, W., Van Larebeke, N., Leijs, M., 2008. Endocrine disruptors and abnormalities of pubertal development. Basic Clin. Pharmacol. Toxicol 102, 168–175. https://doi.org/10.1111/j.1742-7843.2007.00180.x.

Shafei, A., Matbouly, M., Mostafa, E., Al Sannat, S., Abdelrahman, M., Lewis, B., Muhammad, B., Mohamed, S., Mostafa, R.M., 2018. Stop eating plastic, molecular signaling of bisphenol A in breast cancer. Environ. Sci. Pollut. Res. 25, 23624–23630. https://doi.org/10.1007/s11356-018-2540-y.

Sheehan, D.M., 2000. Activity of environmentally relevant low doses of endocrine disruptors and the bisphenol A controversy: Initial Results Confirmed (44515). Exp. Biol. Med. 224, 57–60.

Simian, M., Bissell, M.J., Barcellos-Hoff, M.H., Shyamala, G., 2009. Estrogen and progesterone receptors have distinct roles in the establishment of the hyperplastic phenotype in PR-A transgenic mice. Breast Cancer Res. 11, 1–11. https://doi.org/10.1186/bcr2408.

Sprague, B.L., Trentham-Dietz, A., Hedman, C.J., Wang, J., Hemming, J.D.C., Hampton, J.M., Buist, D.S.M., Aiello Bowles, E.J., Sisney, G.S., Burnside, E.S., 2013. Circulating serum xenoestrogens and mammographic breast density. Breast Cancer Res. 15 https://doi.org/10.1186/bcr3432.

Stein, T., Morris, J.S., Davies, C.R., Weber-Hall, S.J., Duffy, M.-A., Heath, V.J., Bell, A.K., Ferrier, R.K., Sandilands, G.P., Gusterson, B.A., 2003. Involution of the mouse mammary gland is associated with an immune cascade and an acute-phase response, involving LBP, CD14 and STAT3. Breast Cancer Res. 6, R75. https://doi.org/10.1186/bcr753.

Tarullo, S.E., Hill, R.C., Hansen, K.C., Behbod, F., Borges, V.F., Nelson, A.C., Lyons, T.R., 2020. Postpartum breast cancer progression is driven by semaphorin 7a-mediated invasion and survival. Oncogene 39, 2772–2785. https://doi.org/10.1038/s41388-020-1192-9.

Tchou, J., Zhang, P.J., Bi, Y., Satija, C., Marjumdar, R., Stephen, T.L., Lo, A., Chen, H., Mies, C., June, C.H., Conejo-Garcia, J., Puré, E., 2013. Fibroblast activation protein expression by stromal cells and tumor-associated macrophages in human breast cancer. Hum. Pathol. 44, 2549–2557. https://doi.org/10.1016/j.humpath.2013.06.016.

Terry, M.B., Michels, K.B., Brody, J.G., Byrne, C., Chen, S., Jerry, D.J., Malecki, K.M.C., Martin, M.B., Miller, R.L., Neuhausen, S.L., Silk, K., Trentham-Dietz, A., McDonald, J., Oskar, S., Knight, J., Toro-Campos, R., Cai, X., Rising, C.J., Afanaseva, D., Mullis, M.D., Berry, M.P., Bird, J., Bradfield, C., Gangnon, R., Gould, M., Hampton, J., Lindberg, S., Luongo, S., Rolland, B., Shull, J., Gaudet, M., Thornquist, M., Aupperlee, M.D., Haslam, S.Z., Hoshyar, R., Kariagina, A., Lopes, J. R., Miller, K.J., Morozova, O., Newkirk, C.J., Schwartz, R.C., Thomas, B., Totzkay, D., Xie, F., Silk, K.J., Biro, F.M., Fassler, C.S., Giannini, C.M., Pinney, S., Troester, M.A., Burke, K., Herbstman, J., Kehm, R., Lilge, L., Perera, F., Sahay, D., Tehranifar, P., Walker, D., Zeinomar, N., De Hoz, M., Shepard, P., Binder, A., Bessonneau, V., De La Rosa, V., Ohayon, J., Rudel, R., Corvalan, C., Pereira, A., Pereira, J., Russo, J., Yanrong, S., Shepherd, J., Adams-Campbell, L., Dash, C., Haddad, B., Hamilton, R., Richardson, B., Denic-Roberts, H., Chang, G., Ding, Y.C., Kanaya, N., Rakoff, M., Saeki, K., Serrano, M., Reynolds, P., Dunphy, K., Jerry, J., Symington, A., Vandenberg, L., Schneider, S., Adams, S.A., Brandt, H.M., Friedman, D., Lead, J.R., Kreps, G., Wright, K., Burke-Garcia, A., Fisher, C., 2019. Environmental exposures during windows of susceptibility for breast cancer: A framework for prevention research. Breast Cancer Res. 21, 1–16. https://doi.org/10.1186/s13058-019-1168-2.

Vandenberg, L.N., Colborn, T., Hayes, T.B., Heindel, J.J., Jacobs, D.R., Lee, D.H., Shioda, T., Soto, A.M., vom Saal, F.S., Welshons, W.V., Zoeller, R.T., Myers, J.P., 2012. Hormones and endocrine-disrupting chemicals: Low-dose effects and nonmonotonic dose responses. Endocr. Rev. 33, 378–455. https://doi.org/10.1210/er.2011-1050.

vom Saal, F.S., Vandenberg, L.N., 2021. Update on the health effects of bisphenol a: overwhelming evidence of harm. Endocrinology 162, 1–25. https://doi.org/10.1210/endocr/bqaa171.

Wadia, P.R., Cabaton, N.J., Borrero, M.D., Rubin, B.S., Sonnenschein, C., Shioda, T., Soto, A.M., 2013. Low-dose BPA exposure alters the mesenchymal and epithelial transcriptomes of the mouse fetal mammary gland. PLoS One 8. https://doi.org/10.1371/journal.pone.0063902.

Wallace, T.R., Tarullo, S.E., Crump, L.S., Lyons, T.R., 2019. Studies of postpartum mammary gland involution reveal novel pro-metastatic mechanisms. J. Cancer Metastasis Treat. 2019, 139–148. https://doi.org/10.20517/2394-4722.2019.01.

Wang, D., Gao, H., Bandyopadhyay, A., Wu, A., Yeh, I.-T., Chen, Y., Zou, Y., Huang, C., Walter, C.A., Dong, Q., Sun, L.-Z., 2014. Pubertal bisphenol A exposure alters murine mammary stem cell function leading to early neoplasia in regenerated glands. Cancer Prev. Res. 7, 445–455. https://doi.org/10.1158/1940-6207.CAPR-13-0260.

Wang, X., Sun, L., Maffini, M.V., Soto, A., Sonnenschein, C., Kaplan, D.L., 2010. A complex 3D human tissue culture system based on mammary stromal cells and silk scaffolds for modeling breast morphogenesis and function. Biomaterials 31, 3920–3929. https://doi.org/10.1016/j.biomaterials.2010.01.118.

Wani, N.A., Nasser, M.W., Ahirwar, D.K., Zhao, H., Miao, Z., Shilo, K., Ganju, R.K., 2014. C-X-C motif chemokine 12/C-X-C chemokine receptor type 7 signaling regulates breast cancer growth and metastasis by modulating the tumor microenvironment. Breast Cancer Res. 16, 1–17. https://doi.org/10.1186/bcr3665.

Wärri, A., Cook, K.L., Hu, R., Jin, L., Zwart, A., Soto-Pantoja, D.R., Liu, J., Finkel, T., Clarke, R., 2018. Autophagy and unfolded protein response (UPR) regulate mammary gland involution by restraining apoptosis-driven irreversible changes. Cell Death Discov. 4 https://doi.org/10.1038/s41420-018-0105-y.

Watson, C.J., 2006. Key stages in mammary gland development Involution: Apoptosis and tissue remodelling that convert the mammary gland from milk factory to a quiescent organ. Breast Cancer Res 8, 1–5. https://doi.org/10.1186/bcr1401.

Xu, D., dan, Wang, G., He, X. jing, Wang, J. fa, Yang, B., Sun, Z. peng, Sun, D. bo, He, Q. yu, Zhang, X., Wu, R., 2017. 17β-Estradiol and progesterone decrease MDP induced NOD2 expression in bovine mammary epithelial cells. Vet. Immunol. Immunopathol. 188, 59–64. https://doi.org/10.1016/j.vetimm.2017.04.010.

Xu, R., 2017. Mammary epithelial polarity and macrophage infiltration. Macrophage 4, e1521. https://doi.org/10.1016/j.physbeh.2017.03.040.

Yuan, J., Yang, Y., Gao, Z., Wang, Z., Ji, W., Song, W., Zhang, F., Niu, R., 2017. Tyr23 phosphorylation of Anxa2 enhances STAT3 activation and promotes proliferation and invasion of breast cancer cells. Breast Cancer Res. Treat 164, 327–340. https://doi.org/10.1007/s10549-017-4271-z.

Zhang, S., Ekman, M., Thakur, N., Bu, S., Davoodpour, P., Grimsby, S., Tagami, S., Heldin, C.H., Landström, M., 2006. TGFβ1-induced activation of ATM and p53 mediates apoptosis in a Smad7-dependent manner. Cell Cycle 5, 2787–2795. https://doi.org/10.4161/cc.5.23.3523.

Zollo, M., Di Dato, V., Spano, D., De Martino, D., Liguori, L., Marino, N., Vastolo, V., Navas, L., Garrone, B., Mangano, G., Biondi, G., Guglielmotti, A., Yang, L., Huang, J. J., Ren, X., Gorska, A.E., Chytil, A., Aakre, M., Carbone, D.P., Matrisian, L.M.M., Richmond, A., Lin, P.C., Moses, H.L., Wani, N.A., Nasser, M.W., Ahirwar, D.K., Zhao, H., Miao, Z., Shilo, K., Ganju, R.K., Ungari, M., Ferrero, G., Varotti, E., Gusolfino, M.D., Manotti, L., Tanzi, G., Trombatore, M., Bertoni, R., Stein, T., Morris, J.S., Davies, C.R., Weber-Hall, S.J., Duffy, M.A., Heath, V.J., Bell, A.K., Ferrier, R.K., Sandilands, G.P., Gusterson, B.A., Van Dang, H., Sakai, T., Pham, T.A., Tran, D.H., Yorita, K., Shishido, Y., Fukui, K., Ramírez-Valadez, K.A., Vázquez-Victorio, G., Macías-Silva, M., González-Espinosa, C., Jeffrey, W.Pollard, Liu, Y., Mei, C., Liu, H., Wang, H., Zeng, G., Lin, J., Xu, M., Lilla, J.N., Joshi, R.V., Craik, C.S., Werb, Z., Kupferman, M.E., Fini, M.E., Muller, W.J., Weber, R., Cheng, Y., Muschel, R.J., Mendes, L.O., Amorim, J.P.A., Teixeira, G.R., Chuffa, L.G.A., Fioruci, B.A., Pimentel, T.A., de Mello, W., Padovani, C.R., Pereira, S., Martinez, M., Pinheiro, P.F.F., Oliani, S.M., Martinez, F.E., Huang, F.M., Chang, Y.C., Lee, S.S., Yang, M.L., Kuan, Y.H., Gan, L., Qiu, Z., Huang, J.J., Li, Y., Huang, H., Xiang, T., Wan, J., Hui, T., Lin, Y., Li, H., Ren, G., Elgert, K.D., Alleva, D.G., Mullins, D.W., Durando, M., Kass, L., Piva, J., Sonnenschein, C., Soto, A.M., Luque, E.H., Muñoz-De-Toro, M., Dawson, C.A., Pal, B., Vaillant, F., Gandolfo, L.C., Liu, Z., Bleriot, C., Ginhoux, F., Smyth, G.K., Lindeman, G.J., Mueller, S.N., Rios, A.C., Visvader, J.E., Dasari, P., Sharkey, D.J., Noordin, E., Glynn, D.J., Hodson, L.J., Chin, P.Y., Evdokiou, A., Robertson, S.A., Ingman, W.V., Clarkson, R.W.E., Boland, M.P., Kritikou, E.A., Lee, J.M., Freeman, T.C., Tiffen, P.G., Watson, C.J., Clark, N.M., Bos, P.D., Aoki, M., Pawankar, R., Niimi, Y., Kawana, S., Allavena, P., Sica, A., Solinas, G., Porta, C., Mantovani, A., Kanaya, N., Chang, G., Wu, X., Saeki, K., Bernal, L., Shim, H.-J., Wang, J., Warden, C., Yamamoto, T., Li, J., Park, J.-S., Synold, T., Vonderfecht, S., Rakoff, M., Neuhausen, S.L., Chen, S., Dasari, P., Sharkey, D.J., Noordin, E., Glynn, D.J., Hodson, L.J., Chin, P.Y., Evdokiou, A., Robertson, S.A., Ingman, W.V., Allavena, P., Sica, A., Solinas, G., Porta, C., Mantovani, A., Aoki, M., Pawankar, R., Niimi, Y., Kawana, S., Clark, N.M., Bos, P.D., Clarkson, R.W.E., Boland, M.P., Kritikou, E.A., Lee, J.M., Freeman, T.C., Tiffen, P.G., Watson, C.J., Dawson, C.A., Pal, B., Vaillant, F., Gandolfo, L.C., Liu, Z., Bleriot, C., Ginhoux, F., Smyth, G.K., Lindeman, G.J., Mueller, S.N., Rios, A.C., Visvader, J.E., Durando, M., Kass, L., Piva, J., Sonnenschein, C., Soto, A.M., Luque, E.H., Muñoz-De-Toro, M., Elgert, K.D., Alleva, D.G., Mullins, D.W., Gan, L., Qiu, Z., Huang, J.J., Li, Y., Huang, H., Xiang, T., Wan, J., Hui, T., Lin, Y., Li, H., Ren, G., Huang, F.M., Chang, Y.C., Lee, S.S., Yang, M.L., Kuan, Y.H., Mendes, L.O., Amorim, J.P.A., Teixeira, G.R., Chuffa, L.G.A., Fioruci, B.A., Pimentel, T.A., de Mello, W.,

Padovani, C.R., Pereira, S., Martinez, M., Pinheiro, P.F.F., Oliani, S.M., Martinez, F. E., Kupferman, M.E., Fini, M.E., Muller, W.J., Weber, R., Cheng, Y., Muschel, R.J., Lilla, J.N., Joshi, R.V., Craik, C.S., Werb, Z., Liu, Y., Mei, C., Liu, H., Wang, H., Zeng, G., Lin, J., Xu, M., Jeffrey, W.Pollard, Ramírez-Valadez, K.A., Vázquez-Victorio, G., Macías-Silva, M., González-Espinosa, C., Van Dang, H., Sakai, T., Pham, T.A., Tran, D.H., Yorita, K., Shishido, Y., Fukui, K., Stein, T., Morris, J.S., Davies, C.R., Weber-Hall, S.J., Duffy, M.A., Heath, V.J., Bell, A.K., Ferrier, R.K., Sandilands, G.P., Gusterson, B.A., Ungari, M., Ferrero, G., Varotti, E., Gusolfino, M. D., Manotti, L., Tanzi, G., Trombatore, M., Bertoni, R., Wani, N.A., Nasser, M.W., Ahirwar, D.K., Zhao, H., Miao, Z., Shilo, K., Ganju, R.K., Yang, L., Huang, J.J., Ren, X., Gorska, A.E., Chytil, A., Aakre, M., Carbone, D.P., Matrisian, L.M.M., Richmond, A., Lin, P.C., Moses, H.L., Zollo, M., Di Dato, V., Spano, D., De Martino, D., Liguori, L., Marino, N., Vastolo, V., Navas, L., Garrone, B., Mangano, G., Biondi, G., Guglielmotti, A., 2014. Tumor-induced Immune Dysfunction: The Macrophage Connection. In: J. Biol. Chem, 66, pp. 1777–1783. https://doi.org/10.1007/s10585-012-9473-5.